Global critical temperature in disordered superconductors with weak multifractality

James Mayoh and Antonio M. García-García
TCM Group, Cavendish Laboratory, University of Cambridge, JJ Thomson Avenue, Cambridge, CB3 0HE, United Kingdom
(Received 5 March 2015; revised manuscript received 26 October 2015; published 23 November 2015)

There is growing evidence that a key feature of sufficiently disordered superconductors is the spatial inhomogeneity of the order parameter. However, not much is known analytically about the impact of the inhomogeneity on the global critical temperature that signals the onset of resistance in the superconductor. Here we address this problem in the experimentally relevant case of disordered conventional superconductors characterized by weak multifractality such as quasi-two-dimensional thin films. We compute analytically the superconducting energy gap, the temperature at which it vanishes, and the energy dependence and spatial distribution of the order parameter. The latter is found to be log normal. The global critical temperature, computed by percolation techniques, is much smaller than the temperature at which the energy gap vanishes. We show that disorder might enhance superconductivity but only for very weakly coupled superconductors, such as Al, and for relatively weak phase fluctuations. These results are consistent with experiments where enhancement of the critical temperature is observed in Al thin films but not in more strongly coupled materials.

DOI: 10.1103/PhysRevB.92.174526 PACS number(s): 74.78.Na, 74.40.−n, 75.10.Pq

For many years the role of disorder in superconductivity was believed to be well understood. According to the so called Anderson theorem [1], also stated independently by Gor'kov and Abrikosov [2], the critical temperature of a conventional weakly coupled superconductor is not affected by weak nonmagnetic impurity scattering. These results are based on the assumption that the local density of states in the material is unaffected by weak disorder [3,4]. However, with the development of the Bogoliubov–de Gennes theory of superconductivity [5] it became clear that the order parameter becomes increasingly inhomogeneous with increasing disorder.

Experimentally it is well established [6–14], especially for conventional superconducting thin films, that the critical temperature decreases monotonically as disorder increases. Analytic results [15,16], obtained using mesoscopic techniques, confirmed that the interplay between weak disorder and Coulomb interactions could explain this suppression of the critical temperature. For stronger disorder around the superconductor insulator transition there is strong numerical [17,18] evidence that, even in the absence of Coulomb interactions, phase fluctuations are enhanced [19] and the superconducting order parameter becomes highly inhomogeneous [20,21] developing an emergent granularity. Close to the Berezinski-Kosterlitz-Thouless transition phase correlation only persist along a ramified network, reminiscent of a percolation transition [22]. This is consistent with experimental observations of a universal scaling of the order parameter amplitude distribution function [23], granularity [24,25] induced by disorder and reports of glassy features [26], with a supercurrent flow pattern reminiscent of a percolative cluster [27], a pseudogap phase [28,29], and preformed Cooper pairs [30] for sufficiently strong disorder.

The upshot of this discussion is that the order parameter in the presence of strong disorder is highly inhomogeneous with strong phase fluctuations which makes it unlikely that superconductivity can be more robust than in the clean limit. The Anderson theorem does not really apply in this region as self-averaging, one of its assumptions, is not expected to hold for sufficiently strong disorder. However, recent theoretical studies have suggested that enhancement might indeed occur in the presence of strong disorder [31–33]. In Refs. [31,34] it was reported that superconductivity was strongly enhanced around the Anderson metal-insulator transition as a consequence of the strong correlations [35] of the multifractal [36–38] eigenstates of the one-body problem around the Fermi energy. The enhancement still persists [33] even if Coulomb interactions are taken into account perturbatively. These papers employ a simple mean-field BCS formalism that includes explicitly the multifractal correlations of eigenstates. In the region of strong multifractality, relevant for the three-dimensional Anderson transition, the critical temperature, defined in [31,34] as the temperature for which the order parameter at the Fermi energy vanishes, is computed analytically as a function of multifractal exponents, the electron-phonon coupling constant and E_0 a cutoff related to the minimum length scale for which the eigenfunctions are multifractal. For the three-dimensional Anderson transition E_0 is of the order of the Fermi energy of the material. Since the cutoff induced by the Debye energy ϵ_D is neglected in [31,34] the prediction for the critical temperature, proportional to E_0, is rather unrealistic (>1000 K) at least for weakly coupled superconductors. In general this approximation is justified in the context of cold atoms physics or in the limit of very strong multifractality. Another limitation of the results of Refs. [31,34] is that, though the moments of the spatially dependent order parameter were estimated in [34], there is no a precise prediction for the spatial distribution of the order parameter and the local critical temperature.

Despite these shortcomings, the proposal that multifractality might have a profound impact on superconductivity is intriguing and deserves further investigation. Moreover, the recent density matrix renormalization group analysis of Ref. [32], which includes the effect of phase fluctuations, showed that phase coherence in a one-dimensional disordered Hubbard model with attractive interactions at zero temperature is enhanced for weak coupling and disorder close to but below the superconductor-insulator threshold. It is therefore feasible that disorder might, after all, enhance superconductivity but,

most likely, on much more modest scale than suggested in [34].

In this paper we revisit the problem in the limit weak multifractality [38] relevant in a variety of problems: two-dimensional weakly disordered superconductors for system sizes much smaller than the localization length [38], weakly disordered $2+\epsilon$ superconductors in the $\epsilon \ll 1$ limit [36], two-dimensional disordered superconductors with spin-orbit interactions [39], and one-dimensional superconductors with long-range hopping [40]. We first compute exactly the order parameter at the Fermi energy, the energy gap, including explicitly the Debye energy cutoff. In the limit of weak multifractality we compute analytically the energy dependence and the spatial distribution of the order parameter and the local critical temperature. With this information available we compute the critical temperature of the material, defined as the maximum temperature at which a supercurrent can flow, by percolation techniques.

The main conclusions of our work are:

(a) The spatial distribution function of the order parameter, and the associated local critical temperature, is always log normal.

(b) The global critical temperature of the sample, defined as the maximum temperature at which a supercurrent can flow, resulting from a percolation analysis, is very sensitive to the strength of the electron-phonon coupling constant. In all cases the global critical temperature is substantially lower than for a homogeneous order parameter computed at the Fermi energy. We only find an enhancement of this critical temperature, with respect to the bulk nondisordered limit, for very weak electron-phonon coupling.

(c) A crude estimation of the effect of phase fluctuations, induced by the Coulomb interaction or other processes, that suppresses superconductivity shows that in a realistic situation a substantial enhancement of the global critical temperature by disorder might be possible only in very weakly coupled materials such as aluminum. This is in qualitative agreement with the experimental observations of enhancement of the critical temperature in Al thin film [7,41], but not in other more strongly coupled materials, in a region of parameters for which multifractality might be relevant.

The paper is organized as follows. We first introduced in the next section the standard formalism to study inhomogeneous superconductors. In Sec. II we derive exact expressions for the superconducting gap, the critical temperature at the Fermi energy, and its leading energy dependence for disordered superconductors characterized by one-body weakly multifractal eigenstates. Multifractal exponents are directly related to the conductance of the material. Next we calculate analytically the full statistical distribution of the order parameter and the critical temperature in real space. The distribution is always log normal and shows a highly inhomogeneous pattern with emergent granularity as disorder increases in line with the early predictions of Refs. [17,18]. We then compute the global critical temperature by assuming that the transition is induced by percolation. A rough estimation of the suppression of the global critical temperature due to phase fluctuations is then carried out by slightly increasing the percolation threshold. Finally, we discuss the limitations of the model and the relevance of our results for experiments.

I. BCS SUPERCONDUCTIVITY AND INHOMOGENEITIES

The natural framework to study the interplay of superconductivity and inhomogeneities is that of the Bogouliubov–de Gennes (BdG) theory of superconductivity [5,42]. In this formalism the space-dependent mean-field BCS Hamiltonian,

$$H = \int d\mathbf{r}\Bigg[\sum_{\sigma}\Psi_{\sigma}^{\dagger}(\mathbf{r})\left(-\frac{\hbar^2}{2m}\nabla^2 + U(\mathbf{r}) - \mu\right)\Psi_{\sigma}(\mathbf{r}) + \Delta(\mathbf{r})\Psi_{\downarrow}^{\dagger}(\mathbf{r})\Psi_{\uparrow}^{\dagger}(\mathbf{r}) + \text{H.c.}\Bigg], \tag{1}$$

where $\Psi_{\sigma}^{\dagger}(\mathbf{r})$ creates an electron in position eigenstate $\mathbf{r}$ and spin σ and $U(\mathbf{r})$ is the random potential, is diagonalized by the generalized Bogoliubov transformation,

$$\begin{aligned}\Psi_{\uparrow}(\mathbf{r}) &= \sum_{\mathbf{n}}(u_{\mathbf{n}}(\mathbf{r})\gamma_{\uparrow,\mathbf{n}} - v_{\mathbf{n}}^{*}(\mathbf{r})\gamma_{\downarrow,n}^{\dagger}),\\ \Psi_{\downarrow}(\mathbf{r}) &= \sum_{\mathbf{n}}(u_{\mathbf{n}}(\mathbf{r})\gamma_{\downarrow,\mathbf{n}} + v_{\mathbf{n}}^{*}(\mathbf{r})\gamma_{\uparrow,\mathbf{n}}^{\dagger}),\end{aligned} \tag{2}$$

where the coherence factors $v_{\mathbf{n}}(\mathbf{r})$ and $u_{\mathbf{n}}(\mathbf{r})$ depend on the index $\mathbf{n}$ that labels some convenient basis set for the problem. The superconducting state is characterized by the space dependent order parameter $\Delta(\mathbf{r})$,

$$\Delta(\mathbf{r}) = -\frac{\lambda}{\nu(0)}\langle\Psi_{\uparrow}(\mathbf{r})\Psi_{\downarrow}(\mathbf{r})\rangle, \tag{3}$$

where λ is the dimensionless BCS coupling constant and $\nu(0)$ is the bulk density of states at the Fermi energy. One drawback of this approach is that the resulting BdG equations can only be solved numerically. However, it has recently [43,44] been shown numerically that, in the weak coupling limit, it is a good approximation to assume that $u_{\mathbf{n}}(\mathbf{r}), v_{\mathbf{n}}(\mathbf{r})$ are proportional to the eigenstates of the one-body problem $\psi_{\mathbf{n}}(\mathbf{r})$. It is expected that this is only valid in the limit of not very strong spatial inhomogeneities which in our case translates it into a large dimensionless conductance. More specifically, the mean-field approach breaks down when disorder localizes the superconductor in a spatial region whose mean-level spacing is of the order of the bulk superconducting gap. Within this approximation it is straightforward to show that the BdG equations turn into a modified BCS gap equation [1],

$$\Delta(\epsilon) = \frac{\lambda}{2}\int_{-\epsilon_D}^{\epsilon_D}\frac{I(\epsilon,\epsilon')\Delta(\epsilon')}{\sqrt{\epsilon'^2+\Delta^2(\epsilon')}}\tanh\left(\frac{\beta\sqrt{\epsilon'^2+\Delta^2(\epsilon')}}{2}\right)d\epsilon', \tag{4}$$

where ϵ_D is the Debye energy which gives the energetic cutoff for the electron-phonon coupling, $\Delta(\epsilon)$ is the superconducting gap as a function of energy, $\beta = (k_B T)^{-1}$ with T the system temperature, $I(\epsilon,\epsilon') = V\int d\mathbf{r}|\psi(\epsilon,\mathbf{r})|^2|\psi(\epsilon',\mathbf{r})|^2$ are the BCS interaction matrix elements, and $\psi(\epsilon,\mathbf{r})$ is the eigenstate of the one-body problem of energy ϵ. An identical result is obtained from a generalized BCS variational approach. In both cases the spatial dependence of the gap [18,45] is given by

$$\Delta(\mathbf{r}) = \frac{\lambda V}{2}\int\frac{\Delta(\epsilon)}{\sqrt{\Delta(\epsilon)^2+\epsilon^2}}|\psi(\epsilon,\mathbf{r})|^2 d\epsilon. \tag{5}$$

We note that the above formalism for inhomogeneous superconductors has been employed to describe superconductivity

not only in the presence of a disordered potential [31,45] but also in clean confined geometries such as ultrathin films [46], trapped superfluids [47], nanowires [48], and nanograins [49].

From now on we will focus on the problem of superconductivity in a disordered system close to a metal-insulator transition. Several aspects of this problem, including the solution of the gap equation (4) and critical temperature at the Fermi energy [31], the spatial dependence of gap (5) [34] and the role of Coulomb interactions [33] have already been studied in the literature in the limit of strong disorder corresponding to the three-dimensional Anderson transition. The first ingredient necessary to solve the gap equation analytically is an explicit expression for the matrix elements $I(\epsilon,\epsilon')$. By using supersymmetric [38,50], and other nonperturbative techniques, it is possible to find explicit analytic expressions for the matrix elements $I(\epsilon,\epsilon')$ for a broad range of disorder strengths [51]. It is also well established that for disordered systems close to the metal-insulator transition the eigenfunctions are multifractal [51,52]. A commonly used measure for multifractality is the anomalous scaling of the inverse participation ratio (IPR) [36,37],

$$P_q = \int d\mathbf{r}|\psi(\mathbf{r})|^{2q} \sim L^{d_q(q-1)}, \tag{6}$$

where $d_q < d$ is a multifractal dimension. These multifractal exponents also control the slow energy decay of eigenfunction correlations at different energies, namely the matrix elements [35,53],

$$I(\epsilon,\epsilon') = \left(\frac{E_0}{|\epsilon-\epsilon'|}\right)^{\gamma}, \tag{7}$$

so long as $\delta_L \ll |\epsilon-\epsilon'| < E_0$, where $\gamma = 1-\frac{d_2}{d}$ and $\delta_L = 1/\nu(0)L_{\rm loc}^3$ is the mean-level spacing modified by localization effects, $L_{\rm loc}$ is the localization length in the material. The energy scale $E_0 = [\nu(0)L_0^3]^{-1}$ is associated with the large energy cutoff in fractal behavior and L_0 is the short length scale cutoff associated with fractal behavior. Below the metal-insulator transition it is expected L_0 should be of similar size to the mean-free path ℓ. The Ioffe-Regel criterion $k_F\ell \sim 1$ implies that at the mobility edge $E_0 \sim E_F$. In systems with weaker disorder $E_0 \ll E_F$ but typically, at least for weakly coupled metallic superconductors, it is still much larger than other energy scales such as the Debye energy or the superconducting gap.

The parameter $0 \leqslant \gamma \leqslant 1$ describes the strength of multifractality in the system. In particular the scaling exponents d_q depend on the specific model chosen and the degree of disorder. As we mentioned previously, while Refs. [31,34] focused on the strong disordered regime, the results of these paper are only valid in the limit of weak coupling and not very strong spatial inhomogeneities. Weak multifractality, $\gamma \ll 1$, can still occur in this limit, for instance in weakly disordered metals in $2+\epsilon$ dimensions or in strictly two dimensions for sizes much smaller than the localization length. The full set of multifractal dimension in this case is known analytically [38], $d_q \approx d(1-\kappa q)$ with $\kappa = \alpha/g$, g is the dimensionless conductance and $\alpha = 1/2,(1)$ for systems with (broken) time-reversal invariance. We note that for sufficiently large q deviations from this simple linear behavior are expected but these corrections are in general negligible for the observables of interest. The limit $\gamma = 0$ corresponds to zero disorder where the bulk metal behavior is recovered, $I(\epsilon,\epsilon') = 1$ leading to the usual expressions for the BCS gap $\Delta_0 \approx 2\epsilon_D e^{-\frac{1}{\lambda}}$, and the critical temperature $T_{c0} \approx \frac{2e^{\gamma_E}}{\pi}\epsilon_D e^{-\frac{1}{\lambda}}$, where γ_E is the Euler-Mascheroni constant.

We have included explicitly in the gap equation the cutoff, the Debye energy ϵ_D, related to the phonon coupling. This becomes particularly important in the limit $\gamma \to 0$ as the BCS gap equation does not converge for $\epsilon_D \to \infty$. In the limit of weak multifractality, $\gamma \ll 1$, the gap equation is well defined for $\epsilon_D \to \infty$ but we shall see that in order to get meaningful results it is necessary to keep the physical cutoff ϵ_D finite. For $\gamma \approx 1$ it is plausible that the effective cutoff induced by the matrix elements will make ϵ_D less important [31]. However, in this limit the approximation $\Delta \gtrsim \delta_L$ breaks down and the BCS mean-field theory is no longer valid. It should also be noted that the matrix element, Eq. (7), neglects contributions from the region $|\epsilon-\epsilon'| \sim \delta_L$, which will become increasingly important in the case of strong fractality. We show in Appendix A that neglecting the effect of δ_L is valid in the limit of weak multifractality $\gamma \ll 1, \delta_L \ll \epsilon_D$ we are interested in.

II. ENERGY DEPENDENCE OF THE ORDER PARAMETER AT ZERO TEMPERATURE

As a first step to compute analytically, in the limit of weak multifractality $\gamma \ll 1$, the spatial distribution of the order parameter we solve the gap equation at zero temperature,

$$\Delta(\epsilon) = \frac{\lambda}{2}\int_{-\epsilon_D}^{\epsilon_D} \frac{\Delta(\epsilon')}{\sqrt{\epsilon'^2+\Delta^2(\epsilon')}}\left|\frac{E_0}{\epsilon-\epsilon'}\right|^{\gamma} d\epsilon' \tag{8}$$

including its energy dependence. We note that this equation is exactly the same starting point of Refs. [31,34]. Unlike Refs. [31,34], we do take into the account the Debye energy cutoff and compute analytically the full energy dependence of the gap in the weak-multifractality limit.

First we expand the leftmost parts of the gap equation in powers of γ using the ansatz

$$\Delta(\epsilon) = \Delta_\gamma[1+\gamma f_1(\epsilon)+\gamma^2 f_2(\epsilon)+\cdots]. \tag{9}$$

By using standard techniques, detailed in Appendix B, we obtain results for $\Delta_\gamma, f_1(\epsilon), f_2(\epsilon)$. The expansion may be easily continued to arbitrarily high order, however for weak multifractality this is clearly unnecessary. The explicit, but rather cumbersome, analytical expressions for $f_1(\epsilon), f_2(\epsilon)$ Eqs. (B7) and (B10), to be found in Appendix B, are in very good agreement, Fig. 1, with the numerical solution of Eq. (8). We refer to Appendix E for more details on the numerical calculation.

Several comments are in order: (a) The energy dependence of the gap decays smoothly from the Fermi energy with an exponent that depends only on γ. (b) $h_1(\epsilon), h_2(\epsilon)$ are such that $h_i(0) = 0$ and $h_i(\epsilon)$ is an even function in ϵ. This means that $\Delta(0) = \Delta_\gamma(1+\gamma c_1+\gamma^2 c_2)$. The leading correction $c_1 < 0$ is negative as the zeroth order $(E_0/|\epsilon|)^\gamma$ term of the expansion is an overestimation of the exact matrix elements Eq. (7). Increasing E_0 results in smaller c_i and thus the peak of $\Delta(\epsilon)$ is closer to Δ_γ. (c) Unsurprisingly, increasing γ results in a

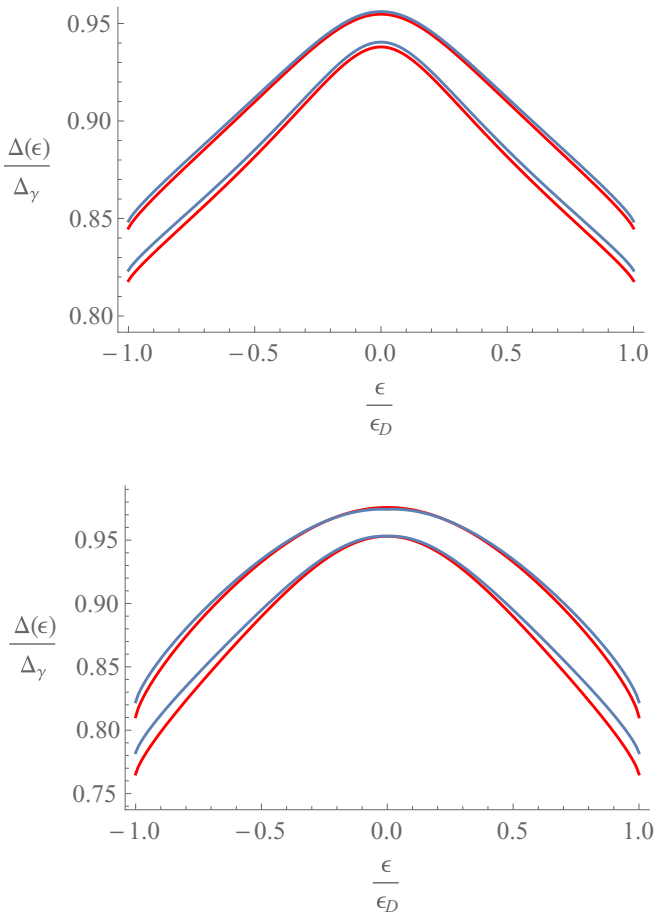

FIG. 1. (Color online) Energy dependence of the gap $\Delta(\epsilon)$. Comparison between the numeric results from Eq. (8) (red) and the analytical calculation $\Delta(\epsilon) = \Delta_\gamma[1 + \gamma f_1(\epsilon) + \gamma^2 f_2(\epsilon)]$ (blue) from Eqs. (B7) and (B10) with $\lambda = 0.3$ and $\gamma = 0.1$ (upper plot) and $\gamma = 0.2$ (lower plot). In both cases the upper pair of lines correspond to $E_0/\epsilon_D = 100$ and the lower pair of lines to $E_0/\epsilon_D = 20$. We observe an excellent agreement in the full range of energy. The decay depends only on the degree of multifractality.

larger error in the analytic results and in a greater difference between the peak value $\Delta(0)$ and the minima $\Delta(\pm\epsilon_D)$.

A. Δ_γ and the associated critical temperature $T_{c\gamma}$

The gap Δ_γ in Eq. (9) is defined as the maximum of the order parameter $\Delta(\epsilon)$ in a disordered system characterized by weak multifractality. It corresponds approximately its value at the Fermi energy. An interesting question to consider in the later study of spatial inhomogeneities and enhancement of superconductivity is how Δ_γ differs from the its value in the clean limit Δ_0.

An exact analytical expression of Δ_γ is available, see Eq. (B6). However, it is more illuminating to carry out an expansion of Eq. (B6) about $\epsilon_D/\Delta_\gamma \to \infty$, a limit that always holds for weakly coupled superconductors and should therefore be valid for $\gamma \ll 1$. Expanding to first order and solving for Δ_γ we find

$$\Delta_\gamma = D(\gamma)\epsilon_D\left[1 + \frac{\gamma}{\lambda}\left(\frac{\epsilon_D}{E_0}\right)^\gamma\right]^{-1/\gamma}, \tag{10}$$

where

$$D(\gamma) = \left(\frac{\gamma\Gamma\left[\frac{1}{2}(1-\gamma)\right]\Gamma\left(\frac{\gamma}{2}\right)}{2\sqrt{\pi}}\right)^{1/\gamma} \tag{11}$$

and $\Gamma(x)$ is the usual Γ function. It should be noted that as $E_0 \to \infty$ the gap Δ_γ is still proportional to ϵ_D, not to E_0 as in [31], where $\Delta_\gamma \sim E_0\lambda^{1/\gamma}$. The reason for this disagreement is that we have kept the Debye energy ϵ_D finite in our calculation. We believe that this is necessary since typically $\epsilon_D \ll E_0$ so it is not consistent to take the Debye energy to infinity while keeping E_0 finite. This is also necessary to recover the BCS result in the limit $\gamma \to 0$, as Eq. (10) does.

In the limit of $\gamma \ll 1$ we can re-express Δ_γ in the more transparent form

$$\Delta_\gamma \approx D(\gamma)\epsilon_D e^{-\frac{1}{\lambda}\left(\frac{\epsilon_D}{E_0}\right)^\gamma}, \tag{12}$$

with $D(\gamma) \approx 2(1 + \frac{\pi^2}{12}\gamma + \cdots)$. This result indicates that in the limit of weak fractality the gap behaves as if it has an effective coupling constant $\lambda_{\text{eff}} = \lambda(\frac{E_0}{\epsilon_D})^\gamma$ giving rise to an exponential increase from Δ_0 with increasing γ, see Fig. 2. This is the reason why even a small value for γ, corresponding to weak disorder, can lead to substantial changes in the superconducting gap with respect to the clean limit provided that the effect of disorder is computed self-consistently.

Another interesting parameter that describes a disordered system is the temperature at which $\Delta(0)$ vanishes. This can be found by solving $1 = \lambda\int_0^{\epsilon_D}(\frac{E_0}{\epsilon})^\gamma\frac{\tanh(\beta_c\epsilon/2)}{\epsilon}d\epsilon$. This integration can also be carried out analytically, see Appendix C, to give

$$k_B T_{c\gamma} = \epsilon_D C(\gamma)\left[1 + \frac{\gamma}{\lambda}\left(\frac{\epsilon_D}{E_0}\right)^\gamma\right]^{-1/\gamma}, \tag{13}$$

where

$$C(\gamma) = [2\gamma(2^{\gamma+1} - 1)\,\Gamma(-\gamma)\,\zeta(-\gamma)]^{1/\gamma} \tag{14}$$

and $\zeta(x)$ is the Riemann ζ function. In the limit $\gamma \to 0$ this expression recovers the BCS result. It should be noted that the derivation of this result is independent from the derivation for Δ_γ.

The ratio of Eqs. (10) and (13), $2\Delta_\gamma/T_{c\gamma}$, is a useful indicator of the relevance of disorder,

$$\frac{2\Delta_\gamma}{k_B T_{c\gamma}} = \frac{2D(\gamma)}{C(\gamma)} = 2\left(\frac{\Gamma\left[\frac{1}{2}(1-\gamma)\right]\Gamma\left(\frac{\gamma}{2}\right)}{4\sqrt{\pi}(2^{\gamma+1} - 1)\,\Gamma(-\gamma)\,\zeta(-\gamma)}\right)^{1/\gamma}. \tag{15}$$

As in the nondisordered case this ratio is independent of the material constants but it is now a function of the strength of the multifractal exponent γ. Expanding about $\gamma = 0$ we find

$$\frac{2\Delta_\gamma}{k_B T_{c\gamma}} = 2\pi e^{-\gamma_E}\left\{1 + \frac{1}{2}\left[\gamma_E^2 - \frac{\pi^2}{12} + 2\ln^2(2) + 2\gamma_1^{sj}\right]\gamma + O(\gamma^2)\right\}, \tag{16}$$

where γ_n^{sj} is the Stieltjes γ function. Note that the BCS result $2\Delta_0/T_{c0} = 2\pi e^{-\gamma_E}$ is recovered in the limit $\gamma \to 0$.

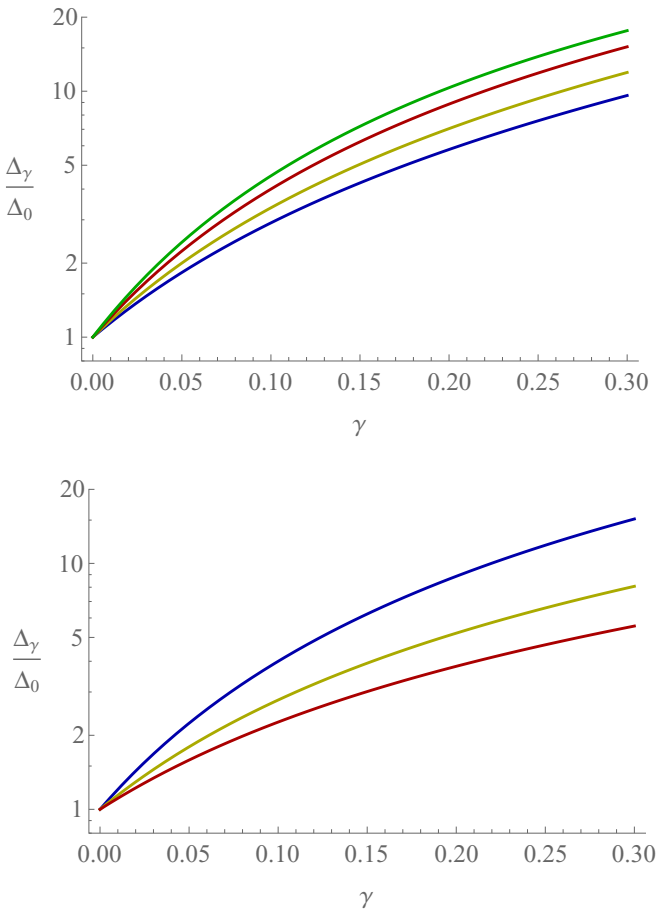

FIG. 2. (Color online) Upper: The value of the gap at the Fermi energy Δ_γ from Eq. (B6) for $\lambda = 0.3$ and $E_0/\epsilon_D = 10$ (blue), 20 (yellow), 50 (red), 100 (green). Lower: $E_0/\epsilon_D = 50$ and $\lambda = 0.3$ (blue), 0.4 (yellow), 0.5 (red). Δ_γ increases exponentially for $\gamma \approx 0$. The gradient decreases for larger γ. We show later that a large value of Δ_γ does not lead necessarily to a large enhancement of the critical temperature of the sample.

The above expression is still valid to relatively large γ as the corrections from higher order terms in the gap and critical temperature are expected to cancel to a good approximation. Indeed Eq. (15) agrees well with recent numerical results focused on the vicinity of $\gamma = 1$ [31], $\frac{2D(\gamma=1)}{C(\gamma=1)} = 4$. However, we refrain from extracting physical conclusions from this limit as the BCS mean-field approach is in principle not applicable. Even in the three-dimensional case $\gamma \approx 0.56$ it is well documented [19] that phase fluctuations, not included in the mean-field approach, play a prominent role. We also note that deviations from the BCS value for the ratio of the gap and critical temperature have been observed experimentally [54]. However, the observable measured in experiment are not defined identically to the theoretical ones above so direct comparison is not trivial. In summary, these results appear to indicate that the gap and critical temperature in a disordered material can be substantially different from that in the clean limit.

The inherent inhomogeneity induced by disorder will play an important role so we expect that both quantities vary substantially in space and therefore we must envisage a procedure to estimate the critical temperature of the sample defined as the maximum temperature for which a supercurrent can flow. To explore these issues we begin by calculating the statistical distribution of the gap in space.

III. DISTRIBUTION OF THE ORDER PARAMETER IN REAL SPACE

In a disordered material the gap in real space is intrinsically inhomogeneous, however for a particular disorder strength it should have a well defined statistical distribution. As was mentioned in the introduction, this spatial distribution function of the order parameter is an outstanding open problem in the theory of superconductivity. In this section we compute analytically this distribution function for the case of weak multifractality of the one-body eigenstates. We leave the details of the calculation to Appendix D and here only sketch the main steps. The starting point is the space dependent gap $\Delta(\mathbf{r})$ Eq. (5), resulting from the generalized trial wave function method mentioned in the introduction, and the energy dependence of the order parameter Eq. (9) computed in the previous section. The moments of $\Delta(\mathbf{r})$ are given by

$$\langle \Delta^n(\mathbf{r}) \rangle = \int d\mathbf{r} \prod_{j=1}^{n} \left(\frac{\lambda V}{2} \int \frac{\Delta(\epsilon_j)}{\sqrt{\Delta(\epsilon_j)^2 + \epsilon_j^2}} |\psi(\epsilon_j, \mathbf{r})|^2 d\epsilon_j \right). \tag{17}$$

In the limit $\gamma \ll 1$, and keeping only leading terms, it is possible to evaluate approximately the generalized eigenstate correlation function above and to compute explicitly the moments. The final result is

$$\frac{\langle \Delta^n(\mathbf{r}) \rangle}{(\Delta_\gamma)^n} = e^{\kappa \ln(\epsilon_D/E_0)(3n-n^2)}, \tag{18}$$

where κ is inversely proportional to the dimensionless conductance $\gamma = 2\kappa$. We note that an explicit expression of $\langle \Delta^n(\mathbf{r}) \rangle$ in the limit of strong multifractality was given in Ref. [34] (Eq. 171).

From Eq. (18) it is straightforward to show that the distribution function associated is log normal,

$$\mathcal{P}\left(\frac{\Delta(\mathbf{r})}{\Delta_\gamma}\right) = \frac{\Delta_\gamma}{\Delta(\mathbf{r})\sqrt{2\pi}\sigma} \exp\left[-\frac{\left[\ln\left(\frac{\Delta(\mathbf{r})}{\Delta_\gamma}\right) - \mu\right]^2}{2\sigma^2} \right], \tag{19}$$

with $\mu = 3\kappa \ln(\epsilon_D/E_0), \sigma = \sqrt{2\kappa \ln(E_0/\epsilon_D)}$. The mean value for the distribution is

$$\left\langle \frac{\Delta(\mathbf{r})}{\Delta_\gamma} \right\rangle = \left(\frac{\epsilon_D}{E_0}\right)^{2\kappa} \tag{20}$$

and the variance is given by

$$\mathrm{Var}\left(\frac{\Delta(\mathbf{r})}{\Delta_\gamma}\right) = \left(\frac{\epsilon_D}{E_0}\right)^{2\kappa} \left[1 - \left(\frac{\epsilon_D}{E_0}\right)^{2\kappa} \right]. \tag{21}$$

As E_0 is typically large compared to ϵ_D the above results indicate that the mean value $\Delta(\mathbf{r})$ can be much smaller than Δ_γ and also that the distribution may be rather broad. These values also indicate that the distribution of $\Delta(\mathbf{r})$ is strongly affected by changes to the disorder strength κ, but is rather weakly dependent on the value of ϵ_D/E_0, see Fig. 3. This

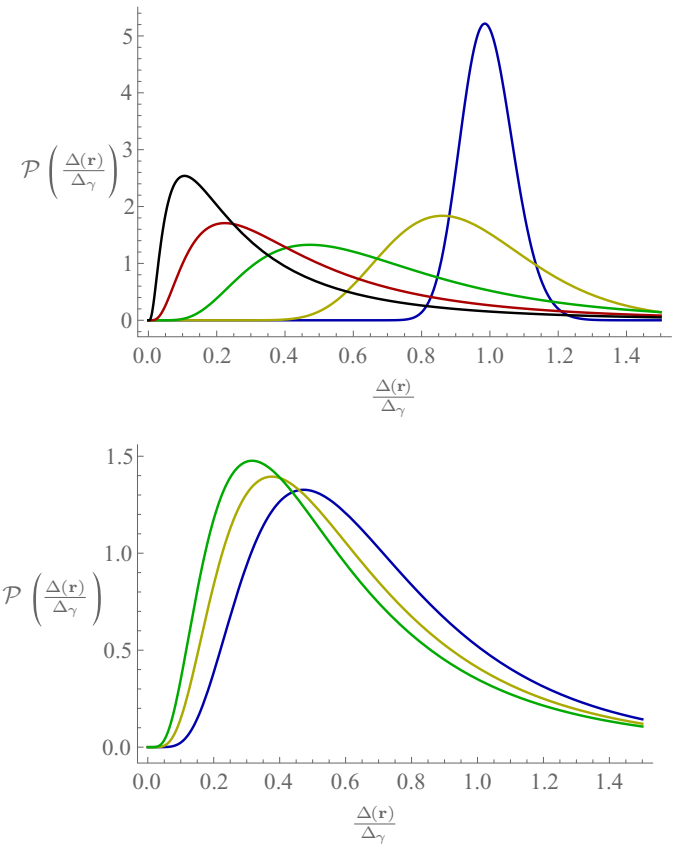

FIG. 3. (Color online) Probability distribution of the gap Eq. (19) for different choices of multifractality strength $\gamma = 2\kappa$ and E_0. Upper: $E_0/\epsilon_D = 20$, $\kappa = 0.001$ (blue), 0.01 (yellow), 0.05 (green), 0.1 (red), 0.15 (black). Lower: $\kappa = 0.05$, $E_0/\epsilon_D = 20$ (blue), 50 (yellow), 100 (green), where κ^{-1} is proportional to the dimensionless conductance (see introduction). In the metallic limit $\kappa \to 0$ the distribution approaches a Dirac δ function centered on the value of the gap at the Fermi energy. For any finite κ the distribution is log normal. It becomes broader as κ increases with a maximum that moves rapidly to smaller values of the gap. The distribution depends only weakly on E_0.

implies that the chosen value of E_0 and any dependence of E_0 on the disorder strength has little effect on our results provided that $\epsilon_D/E_0 \ll 1$.

In the limit $\kappa \to 0$,

$$\mathcal{P}\left(\frac{\Delta(\mathbf{r})}{\Delta_\gamma}\right) = \delta\left(\frac{\Delta(\mathbf{r})}{\Delta_\gamma} - 1\right), \tag{22}$$

this corresponds to the nondisordered case where the gap is uniform in space. Interestingly, as disorder increases, the distribution of the gap broadens and the maximum of the distribution, related to the typical value of the gap, moves to lower values with an extended tail up to $\Delta(\mathbf{r}) > \Delta_\gamma$, see Fig. 3. The decrease in this typical gap value follows physically from the confinement of the electrons to small regions when disorder is added. The gap is enhanced at some points of the material as the single electron wave functions are confined and overlap more strongly. However, the reverse situation also occurs, resulting in many regions where the electron density and gap is reduced compared to the bulk. As disorder strength is increased and the degree of overlap in enhanced regions increases, the area of the suppressed regions also increases resulting in a decrease of the mean value of the distribution. It should be noted that the expansion to higher orders will modify and slightly broaden the distribution of Eq. (19). However, our analytical result still provides a good approximation for the spatial distribution of the gap in the limit of weak multifractality. Indeed it is, see Fig. 3, qualitatively similar to that found in previous numerical and experiment studies [18,23,30].

IV. DISTRIBUTION OF $T_c(\mathbf{r})$

The inverse transformation of Eq. (5) is given by

$$\Delta(\epsilon) = \int d\mathbf{r}\Delta(\mathbf{r})|\psi(\epsilon,\mathbf{r})|^2. \tag{23}$$

In the case of finite temperature this should recover the gap equation Eq. (4). This follows from the generalization of the gap equation at finite temperature,

$$\Delta(\mathbf{r}) = \frac{\lambda V}{2}\int \frac{\Delta(\epsilon)}{\sqrt{\Delta(\epsilon)^2+\epsilon^2}}|\psi(\epsilon,\mathbf{r})|^2 \times \tanh\left(\frac{\sqrt{\epsilon^2+\Delta^2(\epsilon)}}{2k_BT}\right)d\epsilon. \tag{24}$$

It is clear solving for the critical temperature in equation $\Delta(\mathbf{r}) = 0$ for all $\mathbf{r}$ will require that T_c varies in space. We further know $k_BT_c(\epsilon) = \frac{C(\gamma)}{D(\gamma)}\Delta(\epsilon, T=0)$ solves the gap equation Eq. (4) at $\Delta(\epsilon) \to 0$ for all ϵ. It follows that the transformations which apply to the gap must also apply to the critical temperature,

$$T_c(\epsilon) = \int d\mathbf{r}T_c(\mathbf{r})|\psi(\epsilon,\mathbf{r})|^2. \tag{25}$$

By comparison with Eq. (23),

$$k_BT_c(\mathbf{r}) = \frac{C(\gamma)}{D(\gamma)}\Delta(\mathbf{r}, T=0) \tag{26}$$

as one might have expected. Where the distribution function calculated for the gap in space will also hold for the critical temperature,

$$\mathcal{P}\left(\frac{T_c(\mathbf{r})}{T_{c_\gamma}}\right) = \mathcal{P}\left(\frac{\Delta(\mathbf{r})}{\Delta_\gamma}\right). \tag{27}$$

Next we employ this expression as the starting point to estimate the global critical temperature of the material by percolation techniques.

V. CALCULATION OF THE GLOBAL CRITICAL TEMPERATURE OF THE SAMPLE USING A PERCOLATION MODEL

The results from the previous section indicates that weak multifractality is responsible for the broad spatial distribution of the order parameter and the local critical temperature $T_c(\mathbf{r_0})$. This local critical temperature, or the associated local gap, is the natural outcome of a scanning tunneling microscope (STM) experiment. By contrast the temperature at which the order parameter at the Fermi energy, Eq. (10), vanishes is the

spectroscopic gap which can be probed by specific heat or other thermodynamic measurements.

A natural question to ask is: what is the global critical temperature $T_c^{\rm mat}$ of the material defined as the maximum temperature at which a supercurrent can flow? One thing is clear from the previous analysis, $T_c^{\rm mat}$ will be in general much smaller than the temperature at which the spectroscopic gap vanishes. Recent work on inhomogeneous superconductors [22,55] suggest that a percolation transition can be the driving force for the breakdown of phase coherence in an inhomogeneous system. Indeed, many numerical studies have found that at strong disorder and finite temperature phase correlations become in general weakened due to the emergent granularity of the system [17,56,57]. More specifically long-range order is expected to be sustained by the persistence of phase correlations on a ramified network that permeates the system [22].

The global critical temperature $T_c^{\rm mat}$ predicted by percolation of the amplitude of the order parameter neglects two effects: phase fluctuations that can break long-range order even if there exists a percolating cluster for the supercurrent to flow and tunneling between disconnected regions that can induce global long order even if there is no percolating cluster. Both effects have an opposite impact on $T_c^{\rm mat}$ and are relatively small in the limit of weak disorder we are interested in. Therefore, we expect a percolation calculation still provides a good estimation of the temperature at which the loss of long-range order occurs.

Since multifractal eigenstates are scale invariant we find it more natural to employ a continuum percolation model. Therefore, we do not model the sample as a grid of superconducting spots each with a different critical temperature. In a continuum model, disks, or other geometries, are placed randomly in the system. Overlap is of course allowed but the overlapping areas only count towards the critical area fraction once. Thus at the percolation threshold we have a number of areas of the superconducting material which have been built up from a large number of overlapping disks and a number of irregularly shaped nonsuperconducting regions where no disks have been placed. The size of the disks is not important provided that it is much larger than the system size.

The percolation transition occurs when there is sufficient superconducting area $\phi = \phi_c$ so that there exists a superconducting region which completely traverses the surface. The critical temperature of the material $T_c^{\rm mat}$ is thus defined as

$$\int_0^{T_c^{\rm mat}} \mathcal{P}[T_c(\mathbf{r})] dT_c(\mathbf{r}) = 1 - \phi_c. \tag{28}$$

The value of ϕ_c depends weakly on the details of the percolation process. For a two-dimensional surface [58] where the percolation process is induced by placing disks at random positions is $\phi \to \phi_c = 0.676$. Small perturbations to this geometry will not alter substantially ϕ_c. Even for randomly orientated ellipses with aspect ratio two [59] the critical area is still similar $\phi_c = 0.63$. We shall see that $T_c^{\rm mat}$ is robust to small modifications of ϕ_c with respect to $\phi_c = 0.676$. On physical grounds we expect that geometries with just a single typical length must provide a more accurate description of the disordered superconductor. For that reason we employ $\phi = \phi_c = 0.676$ in the next section for explicit calculations of $T_c^{\rm mat}$.

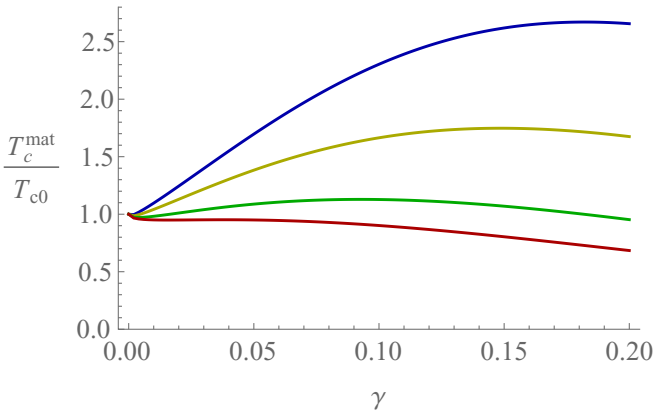

FIG. 4. (Color online) The global critical temperature $T_c^{\rm mat}$, from Eqs. (19) and (28), obtained as the temperature at which the percolation transition occurs, $\phi_c = 0.676$, in units of the BCS nondisordered critical temperature as a function of the degree of multifractality γ for $E_0/\epsilon_D = 100$ and $\lambda = 0.25$ (blue), 0.3 (yellow), 0.4 (green), 0.5 (red). Except in the case of small λ, no or very modest enhancement of $T_c^{\rm mat}$ is observed as γ increases. In all cases $T_c^{\rm mat}$ moves well below $T_{c\gamma}$ [Eq. (13)] due to the distribution of critical temperature becoming increasingly skewed towards smaller values.

Finally, we note the decrease in the mean value of $\mathcal{P}(\frac{T_c(\mathbf{r})}{T_{c\gamma}})$ with increasing disorder suppresses the large exponential enhancement of Δ_γ. The enhancement of the material bulk critical temperature is always much smaller than that of Δ_γ, see Fig. 4. It is only substantially higher than for nondisordered samples in the limit of very small electron-phonon coupling constant that might still describe materials like aluminum. In all other cases we predict a very modest or no enhancement at all is observed.

VI. ESTIMATION OF THE REDUCTION OF THE CRITICAL TEMPERATURE DUE TO PHASE FLUCTUATIONS

An obvious shortcoming of our model is the omission of Coulomb interactions and other sources of phase fluctuations that will reduce significantly the critical temperature of the sample as phase coherence can be lost even above the percolation threshold. Unfortunately a quantitative analytical estimation of these effects is in general quite hard. Even the standard perturbative prediction [15] $\frac{\delta T_c}{T_c} \sim \frac{\lambda_{\rm effec}}{g} \ln^2(\epsilon_D/T_c)$ for the decrease of T_c leaves the final result in terms of the effective strength of the interaction $\lambda_{\rm effec}$, which is in general difficult to estimate especially in a disordered system. The recently developed formalism [55] to address arrays of superconducting nanograins, which includes charging effects, could, at least qualitatively, be adapted to this case. However, it is difficult to estimate rigorously the capacitance in this context. Moreover, we also neglect recombination processes of the order parameter and interactions with single quasiparticles. This is likely a good approximation for low temperatures but for higher temperatures closer to the critical one [60] it is plausible that these processes will effectively broaden the Ginzburg region of

the superconductor and further lower its critical temperature. Again for metallic superconductors it is difficult to make a fully quantitative estimation of the importance of these corrections. Despite these limitations it is clear that phase correlations persist only on an intricate network [22] above the percolation threshold for the amplitude of the order parameter [55]. At least qualitatively it seems therefore plausible that the true global critical temperature of the system $T_c^{\rm mat}$, which includes the effect of phase fluctuations, can still be estimated by percolation techniques by increasing the percolation threshold. This method we apply here to estimate $T_c^{\rm mat}$. For no phase fluctuations the global critical temperature is obtained by setting the fraction ϕ of the superconductor which is above the local critical temperature to the percolation threshold $\phi \approx \phi_c = 0.675$. Therefore, the global critical temperature associated with larger values $\phi > \phi_c$ corresponds to situations where the superconducting fraction is sufficient to support a supercurrent but phase fluctuations prevent phase coherence. We expect the critical area ϕ_c^Q in realistic situations to be higher than the percolation prediction $\phi_c = 0.676$. In Fig. 5 we compare the global critical temperature for different values of ϕ_c^Q, which roughly speaking model the effect of phase fluctuations, and the electron-phonon coupling λ. For sufficiently large λ any enhancement at ϕ_c is rapidly suppressed with increasing disorder. By contrast for sufficiently small λ the enhancement persists even for relatively large values of ϕ_c^Q. We expect the trend of decreasing critical temperature to continue up to stronger disorder, which would agree with the experimental results [6,7]. It is important to stress that this method to mimic the effect of phase fluctuations does not take into account the fact that Coulomb interactions not only induce phase fluctuation but also decrease the superconducting gap and the local critical temperature. Therefore, even the observed substantial enhancement for very weak coupling is only an upper bound of the one that could be observed experimentally.

Clearly a more refined model, beyond the scope of the paper, would be highly desirable to account quantitatively for the effect of phase fluctuations. However, our results suggest that enhancement of the global critical temperature might be possible but only in very weakly coupled superconductors.

VII. RELEVANCE TO EXPERIMENTS

Currently it is feasible to test some of the above theoretical predictions in disordered thin films. Scanning tunneling microscope techniques could be used to measure $\Delta(r_0)$ and $T_c(r_0)$, where the latter is experimentally defined as the temperature for which the gap in the differential conductance vanishes. Indeed the statistical distribution function of the gap, recently measured experimentally in strongly disordered Nb thin films [23] close to the transition, seem qualitatively similar to the log-normal distribution that we have obtained analytically. However, for a quantitative comparison a higher resolution in the experimental results is necessary. Our results could also be employed to measure the multifractal dimensions and the strength of disorder. For instance, according to Eq. (27), the ratio between $\Delta(r_0)$ and $T_c(r_0)$ only depends on the multifractal exponent γ and not on the coupling constant. Experimentally it could be possible to average over r_0 to measure this ratio with better accuracy.

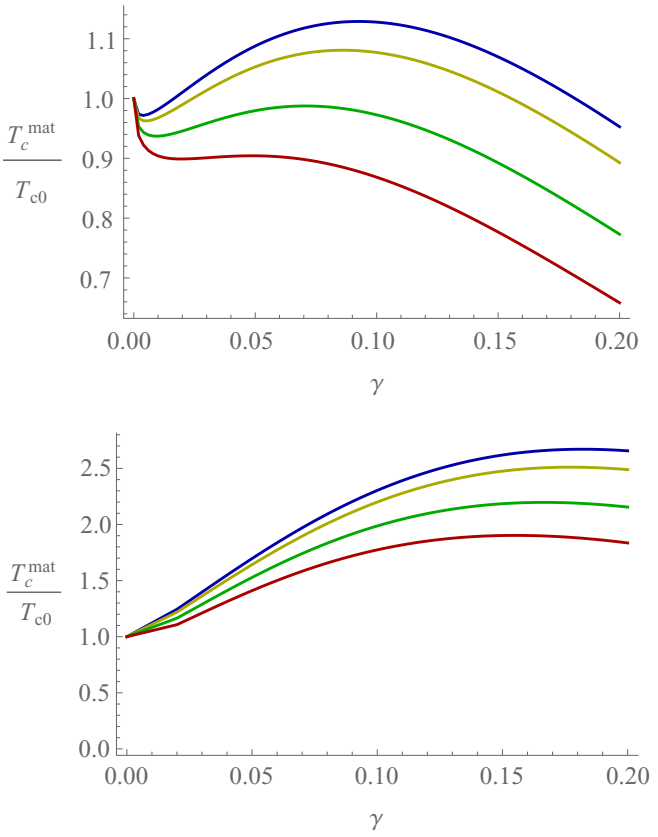

FIG. 5. (Color online) The global critical temperature $T_c^{\rm mat}$ from Eqs. (19) and (28), in units of the clean critical temperature, as a function of the multifractal exponent γ for $E_0/\epsilon_D = 100$, $\lambda = 0.4$ (upper plot) and $\lambda = 0.25$ (lower plot) at the percolation threshold $\phi_c = 0.676$ (blue), and above it, 0.7 (yellow), 0.75 (green), 0.8 (red). An area ϕ_c^Q, greater than the percolation threshold ϕ_c, crudely mimics the effect of phase fluctuations that can break phase coherence even above percolation threshold. The behavior of $T_c^{\rm mat}$ is strongly dependent on the choice of the critical area ϕ_c^Q. We observe that the critical temperature decreases as ϕ_c^Q increases, which for $\lambda = 0.4$ rapidly suppresses any enhancement of the critical temperature with respect to the clean limit. By contrast for $\lambda = 0.25$ a substantial enhancement still occurs even for comparatively large values of ϕ_c^Q. However, this is still an upper bound of the enhancement that can be observed experimentally as we do not take into account the suppression of the order parameter amplitude induced by Coulomb interactions and other processes. Therefore, we expect small or no enhancement except, possibly, for materials such as aluminum that are good metals and have very weak electron-phonon coupling.

Transport measurement like the resistivity could highlight the difference between the local critical temperature $T_c(r_0)$ and the global critical temperature defined as the highest temperature for which a supercurrent can flow. The latter should correspond with our prediction for the global critical temperature $T_c^{\rm mat}$ resulting from the percolation analysis above. Indeed the sharpness of the transition as a function of the temperature could provide important clues on the role of phase fluctuations and percolation of the amplitude in the determination of the global critical temperature.

Specific heat measurements would be a straightforward approach to studying the nature and properties of the phase

transition. In particular the width and height of the peak would supply important information about the superconducting area fraction at the transition and about the distribution function $\mathcal{P}[T(\mathbf{r})]$.

Finally, we stress that one of the main results of the paper, that enhancement of $T_c^{\rm mat}$ by disorder can only be observed in materials with a very weak electron-phonon coupling, is fully consistent with experimental results. It is well known [7,41] that the critical temperature of Al thin films start to increase as the thickness enters in the nanoscale region. By contrast in more strongly coupled superconductors like Pb no enhancement is observed [6,7] and the critical temperature decreases monotonically as the thickness decreases or the disorder strength increases. We note that as the thickness is decreased the material becomes quasi-two-dimensional where multifractality is generic for sufficiently weak disorder. This is the case for metallic superconductors such as Al which are good conductors above the critical temperature.

VIII. CONCLUSIONS

We have studied the interplay between superconductiviy and disorder in a system characterized by weakly multifractal one-body eigenstates. This setting is especially appealing as multifractality enhances pairing correlations and induces strong spatial inhomogeneities in the superconducting order parameter but at the same time it is possible to obtain analytical results. Moreover, weak multifractality is relevant for experiments as it is typical of weakly disordered thin films close to the two-dimensional limit.

First, we have computed exactly the superconducting gap at the Fermi energy, as a function of the multifractal dimensions, and the temperature at which it vanishes. We have found an enhancement of the gap with respect to the clean limit, but much smaller than in recent claims of the literature. Then we have shown that the order parameter is strongly inhomogeneous in space with a distribution function that follows a log-normal distribution. Interestingly the maximum of the distribution deviates strongly from the value of the gap at the Fermi energy as multifractality increases. By using percolation techniques we have found the global critical temperature of the superconductor, defined as the maximum temperature at which a supercurrent can flow, is much lower than the one found by considering the temperature at which the gap at the Fermi energy vanishes. To the best of our knowledge, this is the first time that fully quantitative analytical predictions are derived for the difference between these two temperatures. We note that this is also of direct relevance for experiments as it has recently been observed [30] a finite gap above the global critical temperature in a conventional superconductor. Our formalism does not include directly phase fluctuations, induced by Coulomb interactions or other mechanisms, that further reduce the critical temperature. As a crude method to simulate these effects we have also computed the global critical temperature when the condition for percolation is slightly increased. The outcome of this analysis is that a substantial enhancement of the global critical temperature might be possible only for very weak electron-phonon coupling. This could explain the well known experimental result [7,41] that in aluminum, a material with very weak electron-phonon coupling, the critical temperature is substantially enhanced with respect to the clean limit when the thickness of the sample is sufficiently small. In this limit the material is disordered and quasi-two-dimensional so multifractality plays a role and our formalism is applicable. In addition to disordered thin films close to the two-dimensional limit our results are also relevant for strictly two-dimensional films of size much smaller than the localization length, bulk two-dimensional disordered systems with spin-orbit interactions for which a metal insulator transition occurs in the weak disorder region.

ACKNOWLEDGMENTS

The authors would like to thank Lara Benfatto for useful discussions. A.M.G. would like to thank Sangita Bose and Pratap Raychaudhuri for illuminating discussions. A.M.G. was supported by EPSRC, Grant No. EP/I004637/1, FCT, Grant PTDC/FIS/111348/2009, and a Marie Curie International Reintegration Grant PIRG07-GA-2010-268172. J.M. acknowledges the support of an EPSRC Ph.D. studentship.

APPENDIX A: THE IMPORTANCE OF THE MEAN LEVEL SPACING δ_L ON THE MATRIX ELEMENT

In the work above it is assumed that the matrix element always follows Eq. (7), however the matrix element is known to saturate for states sufficiently close in energy. To see the effect of this saturation we can propose a matrix element which interpolates smoothly between these two behaviors,

$$I(\epsilon,\epsilon') = \left(\frac{E_0}{\sqrt{(\epsilon-\epsilon')^2+\delta_L^2}}\right)^{\gamma} \tag{A1}$$

evaluating about the Fermi energy to zeroth order in γ,

$$1 = \frac{\lambda}{2}\int_{-\epsilon_D}^{\epsilon_D} \frac{1}{\sqrt{\epsilon'^2+\Delta_\gamma^2}}\left(\frac{E_0}{\sqrt{\epsilon^2+\delta_L^2}}\right)^{\gamma} d\epsilon', \tag{A2}$$

$$\frac{1}{\lambda} = \frac{\epsilon_D E_0^{\gamma}}{\Delta_\gamma \delta_L^{\gamma}} F_1\left(\frac{1}{2};\frac{1}{2},\frac{\gamma}{2};\frac{3}{2};-\frac{\epsilon_D^2}{\Delta_\gamma^2},-\frac{\epsilon_D^2}{\delta_L^2}\right), \tag{A3}$$

where F_1 is the Appell hypergeometric function. To compare the results of Eq. (B6) to the results of Eq. (A3) we define

$$R(\delta_L) = \left(\frac{\epsilon_D}{\delta_L}\right)^{\gamma} \frac{(1-\gamma)F_1\left(\frac{1}{2};\frac{1}{2},\frac{\gamma}{2};\frac{3}{2};-\frac{\epsilon_D^2}{\Delta_\gamma^2},-\frac{\epsilon_D^2}{\delta_L^2}\right)}{{}_2F_1\left(\frac{1}{2},\frac{1-\gamma}{2};\frac{3-\gamma}{2};-\frac{\epsilon_D^2}{\Delta_\gamma^2}\right)}. \tag{A4}$$

Such that $R(\delta_L)\sim 1$ implies good agreement between the two forms of the matrix element and the role of δ_L may be neglected. We plot this function for different values of δ_L corresponding to $\delta_L \sim \Delta_{\gamma=0}$ the point at which mean-field BCS treatment breaks down and $\delta_L \ll \Delta_{\gamma=0}$, which is the case for a bulk metal. The later case will hold for $\gamma \ll 1$. We see that in both cases good agreement exists between the two forms of the matrix element up to moderate values of γ. see Fig. 6.

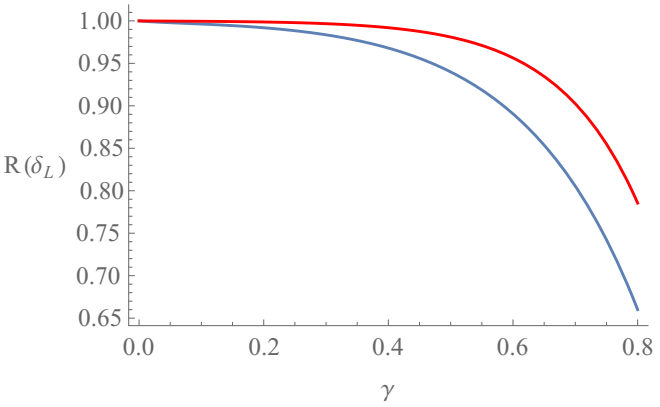

FIG. 6. (Color online) Comparison of $R(\delta_L)$ for $\epsilon_D/\delta_L = 100$ (blue) and $\epsilon_D/\delta_L = 1000$ (red). Corresponding to the limit where BCS mean-field theory breaks down $\delta_L \sim \Delta_{\gamma=0}$, and the case for a clean metal $\delta_L \ll \Delta_{\gamma=0}$, respectively. $R(\delta_L)$ is independent of ϵ_D/E_0 and λ. We note there will be good agreement between results calculated using the simple matrix [Eq. (7)] and results calculated with a careful treatment of the region around δ_L [Eq. (A1)] when $\gamma \ll 1$ and $\delta_L \ll \Delta_0$.

APPENDIX B: ENERGY DEPENDENCE OF THE ORDER PARAMETER AT ZERO TEMPERATURE

The energy dependence of the order parameter is obtained from the following generalized gap equation:

$$\Delta(\epsilon) = \frac{\lambda}{2}\int_{-\epsilon_D}^{\epsilon_D} \frac{\Delta(\epsilon')}{\sqrt{\epsilon'^2+\Delta^2(\epsilon')}}\left|\frac{E_0}{\epsilon-\epsilon'}\right|^{\gamma} d\epsilon', \tag{B1}$$

where we assume that we are in the limit of weak multifractality such that $\gamma \ll 1$. It is not in general acceptable to assume $(\frac{E_0}{|\epsilon|})^{\gamma}$ is small as E_0 may be very large compared to ϵ as discussed in the introduction. For this reason we expand the matrix elements as

$$\begin{aligned} I(\epsilon,\epsilon') &= \left|\frac{E_0}{\epsilon'}\right|^{\gamma} e^{-\gamma \ln\left|1-\frac{\epsilon}{\epsilon'}\right|} \\ &= \left|\frac{E_0}{\epsilon'}\right|^{\gamma}\left(1-\gamma\ln\left|1-\frac{\epsilon}{\epsilon'}\right|+O(\gamma^2)\right), \end{aligned} \tag{B2}$$

the logarithmic terms resulting from this expansion are acceptable as under integration they result in small corrections and so the series is convergent in γ. We can also expand the leftmost parts of the gap equation in powers of γ using the ansatz

$$\Delta(\epsilon) = \Delta_\gamma[1+\gamma f_1(\epsilon)+\gamma^2 f_2(\epsilon)+\cdots]. \tag{B3}$$

For example, to first order in γ,

$$\begin{aligned} &1+\gamma f_1(\epsilon)+O(\gamma^2) \\ &= \frac{\lambda}{2}\int_{-\epsilon_D}^{\epsilon_D}\left(\frac{1}{(\epsilon'^2+\Delta_\gamma^2)^{1/2}}+\gamma\frac{\epsilon'^2 f_1(\epsilon')}{(\epsilon'^2+\Delta_\gamma^2)^{3/2}}+O(\gamma^2)\right) \\ &\quad\times\left|\frac{E_0}{\epsilon'}\right|^{\gamma}\left(1-\gamma\ln\left|1-\frac{\epsilon}{\epsilon'}\right|+O(\gamma^2)\right)d\epsilon'. \end{aligned} \tag{B4}$$

The gap equation can now be solved for Δ_γ, f_1, f_2, and higher terms if necessary, by collecting terms according to their γ dependence.

1. Zeroth order approximation

Collecting the terms of order $|\frac{E_0}{\epsilon'}|^{\gamma}$ we find

$$1 = \frac{\lambda}{2}\int_{-\epsilon_D}^{\epsilon_D}\frac{1}{\sqrt{\epsilon'^2+\Delta_\gamma^2}}\left|\frac{E_0}{\epsilon'}\right|^{\gamma} d\epsilon'. \tag{B5}$$

Carrying out the integral,

$$\frac{1}{\lambda} = \frac{E_0^{\gamma}\epsilon_D^{1-\gamma}}{\Delta_\gamma(1-\gamma)}\,{}_2F_1\left(\frac{1}{2},\frac{1-\gamma}{2};\frac{3-\gamma}{2};-\frac{\epsilon_D^2}{\Delta_\gamma^2}\right), \tag{B6}$$

where ${}_2F_1(a,b;c;d)$ is the hypergeometric function. We define Δ_γ as the solution to this equation which corresponds approximately to the spectroscopic gap, namely, the minimum energy excitation at the Fermi energy. In Sec. II A we will carry out a full analysis of Δ_γ. For now we focus on determining the energy dependence of the gap $\Delta(\epsilon)$.

2. First order approximation

Collecting the terms of order $\gamma|\frac{E_0}{\epsilon'}|^{\gamma}$ from Eq. (B4),

$$\begin{aligned} f_1(\epsilon) = \frac{\lambda}{2}\int_{-\epsilon_D}^{\epsilon_D}\Bigg[&\frac{\epsilon'^2 f_1(\epsilon')}{(\epsilon'^2+\Delta_\gamma^2)^{3/2}}\left|\frac{E_0}{\epsilon'}\right|^{\gamma} \\ &-\frac{\ln\left|1-\frac{\epsilon}{\epsilon'}\right|}{\sqrt{\epsilon'^2+\Delta_\gamma^2}}\left|\frac{E_0}{\epsilon'}\right|^{\gamma}\Bigg]d\epsilon'. \end{aligned} \tag{B7}$$

We solve Eq. (B7) using the ansatz $f_1(\epsilon) = h_1(\epsilon)+c_1$, where c_1 is a constant and we define $h_1(\epsilon)$ as the closed function,

$$h_1(\epsilon) = -\frac{\lambda}{2}\int_{-\epsilon_D}^{\epsilon_D}\frac{\ln\left|1-\frac{\epsilon}{\epsilon'}\right|}{\sqrt{\epsilon'^2+\Delta_\gamma^2}}\left|\frac{E_0}{\epsilon'}\right|^{\gamma} d\epsilon'. \tag{B8}$$

After solving for c_1 we find that the leading correction to Δ_γ is given by

$$f_1(\epsilon) = h_1(\epsilon)+\frac{\frac{\lambda}{2}\int_{-\epsilon_D}^{\epsilon_D}\frac{\epsilon'^2 h_1(\epsilon')}{(\epsilon'^2+\Delta_\gamma^2)^{3/2}}\left|\frac{E_0}{\epsilon'}\right|^{\gamma}d\epsilon'}{1-\frac{\lambda}{2}\int_{-\epsilon_D}^{\epsilon_D}\frac{\epsilon'^2}{(\epsilon'^2+\Delta_\gamma^2)^{3/2}}\left|\frac{E_0}{\epsilon'}\right|^{\gamma}d\epsilon'}. \tag{B9}$$

3. Second order approximation

The treatment for the second order correction $\gamma^2|\frac{E_0}{\epsilon'}|^{\gamma}$ is identical to the first order case. Using a similar ansatz we find

$$\begin{aligned} f_2(\epsilon) = h_2(\epsilon)+&\frac{\frac{\lambda}{2}\int_{-\epsilon_D}^{\epsilon_D}\frac{\epsilon'^2 h_2(\epsilon')}{(\epsilon'^2+\Delta_\gamma^2)^{3/2}}\left|\frac{E_0}{\epsilon'}\right|^{\gamma}d\epsilon'}{1-\frac{\lambda}{2}\int_{-\epsilon_D}^{\epsilon_D}\frac{\epsilon'^2}{(\epsilon'^2+\Delta_\gamma^2)^{3/2}}\left|\frac{E_0}{\epsilon'}\right|^{\gamma}d\epsilon'} \\ &-\frac{3\lambda\Delta_\gamma^2}{4}\int_{-\epsilon_D}^{\epsilon_D}\frac{f_1(\epsilon')^2\epsilon'^2}{(\epsilon'^2+\Delta_\gamma^2)^{5/2}}\left|\frac{E_0}{\epsilon'}\right|^{\gamma}d\epsilon', \end{aligned} \tag{B10}$$

where

$$h_2(\epsilon) = \frac{\lambda}{2}\int_{-\epsilon_D}^{\epsilon_D}\left[\frac{\ln^2\left|1-\frac{\epsilon}{\epsilon'}\right|}{2\sqrt{\epsilon'^2+\Delta_\gamma^2}}\left|\frac{E_0}{\epsilon'}\right|^\gamma - \frac{\epsilon'^2\ln\left|1-\frac{\epsilon}{\epsilon'}\right| f_1(\epsilon')}{\left(\epsilon'^2+\Delta_\gamma^2\right)^{3/2}}\left|\frac{E_0}{\epsilon'}\right|^\gamma\right]d\epsilon'. \quad \text{(B11)}$$

APPENDIX C: DERIVATION OF $T_{c\gamma}$

Starting with

$$1 = \lambda\int_0^{\epsilon_D}\left(\frac{E_0}{\epsilon}\right)^\gamma\frac{\tanh(\beta_c\epsilon/2)}{\epsilon}d\epsilon, \quad \text{(C1)}$$

let $x = \beta\epsilon/2$,

$$1 = \lambda\left(\frac{E_0\beta_c}{2}\right)^\gamma\int_0^{\frac{\beta_c\epsilon_D}{2}}\frac{\tanh(x)}{x^{1+\gamma}}dx. \quad \text{(C2)}$$

We can carry out the integration by rewriting it as

$$\begin{aligned}\int_0^{\frac{\beta_c\epsilon_D}{2}}\frac{\tanh(x)}{x^{1+\gamma}}dx &= \int_0^1\frac{\tanh(x)}{x^{1+\gamma}}dx \\ &\quad+\int_1^{\frac{\beta_c\epsilon_D}{2}}\left(\frac{1}{x^{1+\gamma}}-\frac{2}{x^{1+\gamma}(e^{2x}+1)}\right)dx \\ &= \frac{1}{\gamma}\left[1-\left(\frac{\beta_c\epsilon_D}{2}\right)^{-\gamma}\right]+\int_0^1\frac{\tanh(x)}{x^{1+\gamma}}dx \\ &\quad-\int_1^{\frac{\beta_c\epsilon_D}{2}}\frac{2}{x^{1+\gamma}(e^{2x}+1)}dx. \quad \text{(C3)}\end{aligned}$$

Note the last line is only true if $\gamma \neq 0$. We examine each of the remaining integrals in turn:

$$\int_0^1\frac{\tanh(x)}{x^{1+\gamma}}dx = 2\int_0^1\frac{\sinh(x)}{x^{1+\gamma}}(e^{-x}-e^{-2x}+e^{-5x}-\cdots)dx, \quad \text{(C4)}$$

where we have used $\operatorname{sech}(x) = 2(e^{-x}-e^{-3x}+e^{-5x}-\cdots)$. Integrating term by term and combining the results we find

$$\begin{aligned}&\int_0^1\frac{\tanh(x)}{x^{1+\gamma}}dx \\ &= -\frac{1}{\gamma}+2^{\gamma+1}\Gamma(-\gamma)(1^\gamma-2^\gamma+3^\gamma-\cdots) \\ &\quad+2[\mathrm{E}_{1+\gamma}(2)-\mathrm{E}_{1+\gamma}(4)+\mathrm{E}_{1+\gamma}(6)-\cdots], \quad \text{(C5)}\end{aligned}$$

where $\mathrm{E}_n(x)$ is the exponential integral function

$$\mathrm{E}_n(x) = \int_1^\infty\frac{e^{-xt}}{t^n}dt. \quad \text{(C6)}$$

Note the series $(1^\gamma-2^\gamma+3^\gamma-\cdots)$ is apparently not convergent. We know the integral is convergent and evaluate by taking the analytic continuation,

$$(1^\gamma-2^\gamma+3^\gamma-\cdots) = (1-2^{\gamma+1})\zeta(-\gamma), \quad \text{(C7)}$$

where $\zeta(x)$ is the Riemann ζ function.

Now consider the integral

$$\int_1^{\frac{\beta_c\epsilon_D}{2}}\frac{2}{x^{1+\gamma}(e^{2x}+1)}dx. \quad \text{(C8)}$$

This function is well approximated ($k_BT_c \ll \epsilon_D$) by

$$\begin{aligned}&\int_1^\infty\frac{2}{x^{1+\gamma}(e^{2x}+1)}dx \\ &= \int_1^\infty\frac{\operatorname{sech}(x)e^{-x}}{x^{1+\gamma}}dx \\ &= 2[\mathrm{E}_{1+\gamma}(2)-\mathrm{E}_{1+\gamma}(4)+\mathrm{E}_{1+\gamma}(6)-\cdots]. \quad \text{(C9)}\end{aligned}$$

Combining Eqs. (C3), (C5), (C7), and (C9), and rearranging, gives the result

$$k_BT_c = \epsilon_D C(\gamma)\left[\frac{1}{\lambda}\left(\frac{E_D}{E_0}\right)^\gamma+\frac{1}{\gamma}\right]^{-1/\gamma}, \quad \text{(C10)}$$

$$C(\gamma) = [2(2^{\gamma+1}-1)\,\Gamma(-\gamma)\,\zeta(-\gamma)]^{1/\gamma} \quad \text{(C11)}$$

as required.

APPENDIX D: ANALYTICAL CALCULATION OF THE SPATIAL DISTRIBUTION OF THE ORDER PARAMETER

We begin the calculation of the spatial distribution of the order parameter by computing the moments of $\Delta(\mathbf{r})$ [Eq. (5)],

$$\langle\Delta^n(\mathbf{r})\rangle = \int d\mathbf{r}\prod_{j=1}^n\left(\frac{\lambda V}{2}\int\frac{\Delta(\epsilon_j)}{\sqrt{\Delta(\epsilon_j)^2+\epsilon_j^2}}|\psi(\epsilon_j,\mathbf{r})|^2d\epsilon_j\right), \quad \text{(D1)}$$

where $\Delta(\epsilon_j)$ is given by Eq. (9).

It is clear that in order to proceed it is necessary to evaluate the following correlation function:

$$\tilde{P}_q = V^n\int d\mathbf{r}|\psi(\epsilon_{i_1},\mathbf{r})|^2|\psi(\epsilon_{i_2},\mathbf{r})|^2\cdots|\psi(\epsilon_{i_n},\mathbf{r})|^2. \quad \text{(D2)}$$

An exact analytical solution of Eq. (D1) is not possible, however we shall see that by expanding in $\gamma \ll 1$ and keeping only the leading terms it is possible to find compact analytical solutions.

We assume without loss of generality that $\epsilon_{i_1} > \epsilon_{i_2} > \cdots > \epsilon_{i_n}$ and further always work in the case where $|\epsilon_{i_1}-\epsilon_{i_2}| \approx |\epsilon_{i_2}-\epsilon_{i_3}| \approx \cdots \approx |\epsilon_{i_{n-1}}-\epsilon_{i_n}|$. When the energy separation between the neighboring eigenfunctions is small $|\epsilon_{i_{k-1}}-\epsilon_{i_k}| \sim \delta_L$ we recover the results for the IPR,

$$\tilde{P}_q \sim L^{d_q(q-1)}, \quad \text{(D3)}$$

whereas in the opposite limit $|\epsilon_{i_{k-1}}-\epsilon_{i_k}| \sim E_0$ the eigenfunctions become statistically independent and therefore,

$$\tilde{P}_q \approx V^{2n}\int d\mathbf{r}_1\cdots\int d\mathbf{r}_n|\psi(\epsilon_{i_1},\mathbf{r}_1)|^2\cdots|\psi(\epsilon_{i_n},\mathbf{r}_n)|^2 \sim 1. \quad \text{(D4)}$$

Analogously to the derivation of Eq. (7), the scaling between these two limits can be approximated by

$$\tilde{P}_q \sim \prod_{j=1}^{n-1}\left(\frac{E_0}{|\epsilon_j-\epsilon_{j+1}|}\right)^{\gamma_n}, \quad \text{(D5)}$$

where $\gamma_n = 1 - \frac{d_n}{d}$. The moments of the gap in real space can then be calculated from

$$\langle \Delta^n(\mathbf{r}) \rangle = \frac{\lambda}{2} \int d\epsilon_n \frac{\Delta(\epsilon_n)}{\sqrt{\Delta(\epsilon_n)^2 + \epsilon_n^2}} \times \left[\prod_{j=1}^{n-1} \frac{\lambda}{2} \int d\epsilon_j \frac{\Delta(\epsilon_j)}{\sqrt{\Delta(\epsilon_j)^2 + \epsilon_j^2}} \left(\frac{E_0}{|\epsilon_j - \epsilon_{j+1}|} \right)^{\gamma_n} \right]. \tag{D6}$$

As when we solved the gap equation we expand in γ. We consider the lowest order in γ using $\Delta(\epsilon) = \Delta_\gamma$,

$$\langle \Delta^n(\mathbf{r}) \rangle = \left(\frac{\lambda}{2} \right)^n \left[\prod_{j=1}^{n-1} \int d\epsilon_j \frac{\Delta_\gamma}{\sqrt{\Delta_\gamma^2 + \epsilon_j^2}} \left(\frac{E_0}{|\epsilon_j|} \right)^{\gamma_n} \right] \times \int d\epsilon_n \frac{\Delta(\epsilon_n)}{\sqrt{\Delta(\epsilon_n)^2 + \epsilon_n^2}}. \tag{D7}$$

Carrying out the integrals, and applying Eq. (12), we find

$$\langle \Delta^n(\mathbf{r}) \rangle = (\Delta_\gamma)^n \left(\frac{\epsilon_D}{E_0} \right)^{(\gamma - \gamma_n)(n-1) + \gamma}. \tag{D8}$$

As was discussed in the introduction for a wide range of different systems, for example disorder in $d = 2 + \epsilon$ dimensions, it has been shown that the fractal dimension behaves like $d_n = d(1 - \kappa n)$ [38,51,61], where κ^{-1} is proportional to the dimensionless conductance in the material. This dependence on n applies for all n less than some critical value n_c. For the systems we are interested in, this critical value is sufficiently large that the shape of the distribution will be well described by considering $d_n = d(1 - \kappa n)$ for all n, as modifications to this value only affect very high order moments of the distribution.

Applying this result we can write our moments in the normalized form

$$\frac{\langle \Delta^n(\mathbf{r}) \rangle}{(\Delta_\gamma)^n} = e^{\kappa \ln(\epsilon_D/E_0)(3n - n^2)} \tag{D9}$$

from which it is trivial to write down the characteristic function associated with the distribution of $\Delta(\mathbf{r})/\Delta_\gamma$,

$$\phi(t) = \sum_{n=0}^{\infty} \frac{(it)^n}{n!} e^{\kappa \ln(\epsilon_D/E_0)(3n - n^2)}. \tag{D10}$$

By inspection, this is the characteristic function for a log-normal distribution,

$$\mathcal{P}\left(\frac{\Delta(\mathbf{r})}{\Delta_\gamma} \right) = \frac{\Delta_\gamma}{\Delta(\mathbf{r})\sqrt{2\pi}\sigma} \exp\left[-\frac{\left[\ln\left(\frac{\Delta(\mathbf{r})}{\Delta_\gamma} \right) - \mu \right]^2}{2\sigma^2} \right], \tag{D11}$$

with $\mu = 3\kappa \ln(\epsilon_D/E_0), \sigma = \sqrt{2\kappa \ln(E_0/\epsilon_D)}$. The mean value for the distribution is

$$\left\langle \frac{\Delta(\mathbf{r})}{\Delta_\gamma} \right\rangle = \left(\frac{\epsilon_D}{E_0} \right)^{2\kappa} \tag{D12}$$

and the variance is given by

$$\mathrm{Var}\left(\frac{\Delta(\mathbf{r})}{\Delta_\gamma} \right) = \left(\frac{\epsilon_D}{E_0} \right)^{2\kappa} \left[1 - \left(\frac{\epsilon_D}{E_0} \right)^{2\kappa} \right]. \tag{D13}$$

APPENDIX E: SOLVING THE GAP EQUATION NUMERICALLY

In principle, solving the integral equation (8) is a difficult computational problem. We have developed a simple inexpensive algorithm to do this.

We first define an array of $n = 200$ points ϵ_j equally spaced between $-\epsilon_D$ and ϵ_D. We also define the gap at each of these points $\Delta_{i=0}(\epsilon_j)$ initialized it with a constant value Δ_0. We then define a function which makes the array of the gap into a continuous function $\Delta_{i=0}(\epsilon)$ using a high order polynomial interpolation. The integration can then be carried out using a standard numerical integration algorithm. We calculate $\Delta_{i=1}(\epsilon_j)$ using

$$\Delta_{i+1}(\epsilon_j) = \frac{\lambda}{2} \int_{-\infty}^{\infty} \frac{\Delta_i(\epsilon')}{\sqrt{\epsilon'^2 + \Delta_i^2(\epsilon')}} \left(\frac{E_0}{|\epsilon_j - \epsilon'|} \right)^{\gamma} d\epsilon'. \tag{E1}$$

Now we iterate using $\Delta_{i=1}(\epsilon_j)$ as the input to the interpolation step. After several iterations the results converge to the correct value of the gap. We test convergence by defining the relative error,

$$\mathrm{err}_i = \frac{\sum_j |\Delta_i(\epsilon_j) - \Delta_{i-1}(\epsilon_j)|}{n\Delta_0} \tag{E2}$$

and take convergence to have been reached when $\mathrm{err}_i < 10^{-6}$.

[1] P. W. Anderson, J. Phys. Chem. Solids **11**, 26 (1959).
[2] A. A. Abrikosov and L. P. Gorkov, J. Exp. Theor. Phys. **12**, 1243 (1961).
[3] Y.-J. Kim and A. W. Overhauser, Phys. Rev. B **47**, 8025 (1993).
[4] A. A. Abrikosov and L. P. Gorkov, Phys. Rev. B **49**, 12337 (1994).
[5] P. de Gennes, Rev. Mod. Phys. **36**, 225 (1964).
[6] D. B. Haviland, Y. Liu, and A. M. Goldman, Phys. Rev. Lett. **62**, 2180 (1989).
[7] Y. Liu, D. B. Haviland, B. Nease, and A. M. Goldman, Phys. Rev. B **47**, 5931 (1993).
[8] N. Nishida, M. Yamaguchi, T. Furubayashi, K. Morigaki, H. Ishimoto, and K. Ono, Solid State Commun. **44**, 305 (1982).
[9] T. Furubayashi, N. Nishida, M. Yamaguchi, K. Morigaki, and H. Ishimoto, Solid State Commun. **55**, 513 (1985).
[10] N. Alekseevskii, A. Mitin, V. Samosyuk, and V. Firsov, J. Exp. Theor. Phys. **58**, 635 (1983).
[11] D. Bishop, E. Spencer, and R. Dynes, Solid. State. Electron. **28**, 73 (1985).
[12] J. Graybeal, Phys. B+C **135**, 113 (1985).
[13] E. F. C. Driessen, P. C. J. J. Coumou, R. R. Tromp, P. J. de Visser, and T. M. Klapwijk, Phys. Rev. Lett. **109**, 107003 (2012).

[14] H. Tashiro, J. M. Graybeal, D. B. Tanner, E. J. Nicol, J. P. Carbotte, and G. L. Carr, Phys. Rev. B **78**, 014509 (2008).
[15] S. Maekawa and H. Fukuyama, J. Phys. Soc. Jpn. **51**, 1380 (1982).
[16] S. Maekawa, H. Ebisawa, and H. Fukuyama, J. Phys. Soc. Jpn. **53**, 2681 (1984).
[17] A. Ghosal, M. Randeria, and N. Trivedi, Phys. Rev. Lett. **81**, 3940 (1998).
[18] A. Ghosal, M. Randeria, and N. Trivedi, Phys. Rev. B **65**, 014501 (2001).
[19] M. Mondal, A. Kamlapure, M. Chand, G. Saraswat, S. Kumar, J. Jesudasan, L. Benfatto, V. Tripathi, and P. Raychaudhuri, Phys. Rev. Lett. **106**, 047001 (2011).
[20] N. Trivedi, Y. L. Loh, K. Bouadim, and M. Randeria, J. Phys. Conf. Ser. **376**, 012001 (2012).
[21] D. Sherman, B. Gorshunov, S. Poran, N. Trivedi, E. Farber, M. Dressel, and A. Frydman, Phys. Rev. B **89**, 035149 (2014).
[22] A. Erez and Y. Meir, Phys. Rev. Lett. **111**, 187002 (2013).
[23] G. Lemarié, A. Kamlapure, D. Bucheli, L. Benfatto, J. Lorenzana, G. Seibold, S. C. Ganguli, P. Raychaudhuri, and C. Castellani, Phys. Rev. B **87**, 184509 (2013).
[24] C. Brun, T. Cren, V. Cherkez, F. Debontridder, S. Pons, D. Fokin, M. Tringides, S. Bozhko, L. Ioffe, B. Altshuler *et al.*, Nat. Phys. **10**, 444 (2014).
[25] Y. Noat, V. Cherkez, C. Brun, T. Cren, C. Carbillet, F. Debontridder, K. Ilin, M. Siegel, A. Semenov, H.-W. Hübers, and D. Roditchev, Phys. Rev. B **88**, 014503 (2013).
[26] L. B. Ioffe and M. Mézard, Phys. Rev. Lett. **105**, 037001 (2010).
[27] G. Seibold, L. Benfatto, C. Castellani, and J. Lorenzana, Phys. Rev. Lett. **108**, 207004 (2012).
[28] K. Bouadim, Y. L. Loh, M. Randeria, and N. Trivedi, Nat. Phys. **7**, 884 (2011).
[29] M. Mondal, A. Kamlapure, S. C. Ganguli, J. Jesudasan, V. Bagwe, L. Benfatto, and P. Raychaudhuri, Sci. Rep. **3**, 1357 (2013).
[30] B. Sacépé, T. Dubouchet, C. Chapelier, M. Sanquer, M. Ovadia, D. Shahar, M. Feigel'man, and L. Ioffe, Nat. Phys. **7**, 239 (2011).
[31] M. V. Feigel'man, L. B. Ioffe, V. E. Kravtsov, and E. A. Yuzbashyan, Phys. Rev. Lett. **98**, 027001 (2007).
[32] M. Tezuka and A. M. Garcia-Garcia, Phys. Rev. A **82**, 043613 (2010).
[33] I. S. Burmistrov, I. V. Gornyi, and A. D. Mirlin, Phys. Rev. Lett. **108**, 017002 (2012).
[34] M. V. Feigel'man, L. B. Ioffe, V. E. Kravtsov, and E. Cuevas, Ann. Phys. (NY). **325**, 1390 (2010).
[35] Y. V. Fyodorov and A. D. Mirlin, Phys. Rev. B **55**, R16001 (1997).
[36] F. Wegner, Z. Phys. B Condens. Matter **36**, 209 (1980).
[37] C. Castellani and L. Peliti, J. Phys. A. Math. Gen. **19**, L429 (1986).
[38] V. I. Fal'ko and K. B. Efetov, Europhys. Lett. **32**, 627 (1995).
[39] S. Hikami, A. I. Larkin, and Y. Nagaoka, Prog. Theor. Phys. **63**, 707 (1980).
[40] A. M. Lobos, M. Tezuka, and A. M. Garcia-Garcia, Phys. Rev. B **88**, 134506 (2013).
[41] B. Abeles, R. W. Cohen, and G. W. Cullen, Phys. Rev. Lett. **17**, 632 (1966).
[42] P. de Gennes, *Superconductivity of Metals and Alloys* (W. A. Benjamin, New York, 1966).
[43] A. A. Shanenko, M. D. Croitoru, and F. M. Peeters, Phys. Rev. B **78**, 024505 (2008).
[44] Y. Chen, M. Croitoru, A. Shanenko, and F. Peeters, J. Phys.: Condens. Matter **21**, 435701 (2009).
[45] M. Ma and P. A. Lee, Phys. Rev. B **32**, 5658 (1985).
[46] J. M. Blatt and C. J. Thompson, Phys. Rev. Lett. **10**, 332 (1963).
[47] H. Heiselberg, Phys. Rev. A **68**, 053616 (2003).
[48] A. A. Shanenko, M. D. Croitoru, M. Zgirski, F. M. Peeters, and K. Arutyunov, Phys. Rev. B **74**, 052502 (2006).
[49] A. M. García-García, J. D. Urbina, E. A. Yuzbashyan, K. Richter, and B. L. Altshuler, Phys. Rev. Lett. **100**, 187001 (2008).
[50] K. Efetov, Adv. Phys. **32**, 53 (1983).
[51] A. Mirlin, Phys. Rep. **326**, 259 (2000).
[52] F. Evers and A. Mirlin, Rev. Mod. Phys. **80**, 1355 (2008).
[53] J. Chalker, Phys. A Stat. Mech. Appl. **167**, 253 (1990).
[54] B. Sacépé, C. Chapelier, T. I. Baturina, V. M. Vinokur, M. R. Baklanov, and M. Sanquer, Phys. Rev. Lett. **101**, 157006 (2008).
[55] J. Mayoh and A. M. García-García, Phys. Rev. B **90**, 134513 (2014).
[56] Y. Dubi, Y. Meir, and Y. Avishai, Nature (London) **449**, 876 (2007).
[57] S. Ghosh and S. S. Mandal, Phys. Rev. Lett. **111**, 207004 (2013).
[58] J. A. Quintanilla and R. M. Ziff, Phys. Rev. E **76**, 051115 (2007).
[59] W. Xia and M. F. Thorpe, Phys. Rev. A **38**, 2650 (1988).
[60] A. Kapitulnik and G. Kotliar, Phys. Rev. Lett. **54**, 473 (1985).
[61] F. Evers and A. D. Mirlin, Phys. Rev. Lett. **84**, 3690 (2000).